ImmunoTargets and Therapy

Dovepress
open access to scientific and medical research

Open Access Full Text Article

ORIGINAL RESEARCH

Deciphering Natural Killer Cell Cytotoxicity Against Medulloblastoma in vitro and in vivo: Implications for Immunotherapy

Melanie Gauthier[1,2], Julien Pierson[3], David Moulin[1], Manon Mouginot[1], Valerie Bourguignon[1], Wassim Rhalloussi[1], Jean-Baptiste Vincourt[1], Dominique Dumas[1], Danièle Bensoussan[1,2], Pascal Chastagner[1,4], Cédric Boura[3], Veronique Decot[1,2]

[1]CNRS UMR 7365 IMoPA, Université de Lorraine, Nancy, France; [2]Cell Therapy and Tissue Bank Unit, Nancy University Hospital, Vandoeuvre-Les-Nancy, France; [3]CNRS UMR7039 CRAN, Université de Lorraine, Nancy, France; [4]Pediatric Oncology Department, Nancy University Hospital, Vandoeuvre-Les-Nancy, France

Correspondence: Veronique Decot, CNRS UMR 7365, IMoPA, Campus Brabois Santé, 9 av de la foret de Haye, Vandoeuvre-Les-Nancy, 54000, France, Tel +0033 – 649574720, Email veronique.decot@univ-lorraine.fr

Video abstract

Point your SmartPhone at the code above. If you have a QR code reader the video abstract will appear. Or use: https://youtu.be/g6H8yg1fq1g

Purpose: Medulloblastoma (MB) is the most prevalent paediatric brain tumour. Despite improvements in patient survival with current treatment strategies, the quality of life of these patients remains poor owing to the sequelae and relapse risk. An alternative, or, in addition to the current standard treatment, could be considered immunotherapy, such as Natural Killer cells (NK). NK cells are cytotoxic innate lymphoid cells that play a major role in cancer immunosurveillance. To date, the mechanism of cytotoxicity of NK cells, especially regarding the steps of adhesion, conjugation, cytotoxic granule polarisation in the cell contact area, perforin and granzyme release in two and three dimensions, and therapeutic efficacy in vivo have not been precisely described.

Materials and Methods: Each step of NK cytotoxicity against the three MB cell lines was explored using confocal microscopy for conjugation, Elispot for degranulation, flow cytometry, and luminescence assays for target cell necrosis and lysis and mediators released by cytokine array, and then confirmed in a 3D spheroid model. Medulloblastoma-xenografted mice were treated with NK cells. Their persistence was evaluated by flow cytometry, and their efficacy in tumour growth and survival was determined. In addition, their effects on the tumour transcriptome were evaluated.

Results: NK cells showed variable affinities for conjugation with MB target cells depending on their subgroup and cytokine activation. Chemokines secreted during NK and MB cell co-culture are mainly associated with angiogenesis and immune cell recruitment. NK cell cytotoxicity induces MB cell death in both 2D and 3D co-culture models. NK cells initiated an inflammatory response in a human MB murine model by modulating the MB cell transcriptome.

Conclusion: Our study confirmed that NK cells possess both in vitro and in vivo cytotoxic activity against MB cells and are of interest for the development of immunotherapy.

Keywords: cancer, medulloblastoma, immune cells, adoptive transfer

Introduction

Medulloblastoma (MB) accounts for 10–20% of paediatric brain tumours, is The WHO prevalent brain tumour in children.[1] The disease is classified into four histological groups (anaplastic, desmoplastic, large cell, and extensive nodularity). In 2012, however, a new classification was designed based on molecular patterns, wherein MB was divided into subgroups, namely SHH, Wnt, group 3 and group 4.[2,3]

The current standard treatments include surgery, high-dose chemotherapy, and/or craniospinal radiation therapy. Although these treatments improve survival, the long-term neuroendocrine and intellectual sequelae in these patients remain dramatic.[4] In addition, the chances of recovery are low, especially for high-risk forms (initial metastasis, post-surgical residue, and MYC-N

Received: 5 January 2024
Accepted: 21 May 2024
Published: 26 June 2024

amplification) due to metastases in or outside the central nervous system. Thus, it has a 5 year survival rate of 30–70% of the cases depending on the MB subtype.[1] Hence, there is an urgent need for new therapeutic strategies.[5] Cellular immunotherapies have been shown to be effective in eliminating brain tumour cells while sparing healthy adjacent tissues. One approach that has been considered for the treatment of MB is allogeneic immunotherapy based on T and Natural Killer (NK) cells. T cells are good candidates for MB because of their ability to penetrate the blood-brain barrier.[6] In addition, CAR-T cells have now joined the race for MB immunotherapy and are currently under investigation in Phase I clinical trials (NCT041085038). However, allogeneic T cells may not be the best option because of the risk of graft-versus-host disease, and CAR-T cell infusions are often followed by severe adverse events.[7]

One alternative could be Natural Killer (NK) cells, which are innate lymphoid cells that have attracted interest for MB immunotherapy. As such, they offer numerous advantages, such as their ability to recognise and kill tumour cells without antigen presentation and exert antibody-dependent cellular cytotoxicity via Fcγ receptor expression. NK cells also have a good safety profile, as evidenced in several clinical trials, suggesting their use in off-the-shelf immunotherapies.

NK cells are regulated by a dynamic balance between a wide array of activating and inhibitory receptors that recognise ligands expressed by target cells. The Activating receptors include NKG2D, which recognises MICA/B and ULBP1 expressed by MB[8,9] and receptors belonging to the natural cytotoxicity receptors (NCR) such as NKp30, NKp44, and NKp46. Other receptors expressed by NK cells, such as DNAM-1, which recognises CD155/PVR, are also involved in MB recognition. Although the interaction between NK cells and MB has been previously explored in vitro using MB cell lines,[8] the mechanism of NK cell cytotoxicity has not been precisely described, especially regarding the steps of adhesion, conjugation, cytotoxic granule polarisation, and release in the cell contact area. Furthermore, the antitumour efficacy of NK cells against MB in vivo is poorly explored.

In this study, we focused on deciphering the main steps by which NK cells kill MB using cell lines to represent the main subtypes of MB as targets. Herein, we show the benefits of NK cell therapy combined with IL-15 administration in a heterotopic nude mouse model.

Materials and Methods

NK cells cytotoxicity against MB cells occurs through a succession of several coordinated steps. First of all, conjugation, allowing the recognition and attachment of the NK cell membrane to its target via the immunological synapse, was assessed using confocal microscopy. The expression of the ligand/receptor pairs involved in the synapse was studied using flow cytometry. Then, the release cytokines and chemokines following activation was detected in the surrounding environment by cytokine array technique. Finally, the release of granzymes from the cytotoxic granules inducing target cells lysis was measured by ELISPOT assay. Target cell death was observed in 2D and 3D co-culture models, using flow cytometry and microscopy. The in-vitro results were then confirmed in a mouse model of human MB.

Cell Lines

DAOY (HTB-186™), D283 (HTB-185™), and D341 (HTB-187™) human MB cell lines were obtained from the ATCC. DAOY and D283 cells were cultured in MEM (Gibco) supplemented with L-glutamine (Eurobio), sodium pyruvate (1 mM, Gibco, USA), non-essential amino acids (1 mM, Gibco), and 10% foetal calf serum (FCS, Gibco). D341 cells were cultured with 20% FCS. The K562 cell line was obtained from ATCC (USA) and cultured in RPMI medium supplemented with 20% foetal calf serum (FCS).

3D DAOY Spheroid Model

DAOY cells were seeded on an ultra-low attachment (ULA) plate (Nunclon™, Thermo Fisher) at various densities. Spheroid diameter and morphology were assessed using an inverted brightfield microscope (Eclipse TS100, Nikon) under x4 or x10 magnifying, and imaged using a Nikon DS Fi1 (Nikon) camera on NIS elements F3.2. Spheroid measurements were performed using ImageJ software.

NK Cell Enrichment, Culture and Freezing

NK cells were obtained from peripheral blood mononuclear cells (PBMCs) obtained from healthy human donors after informed consent (EFS Grand-Est). Fresh unstimulated NK cells were enriched with the LS MACS separation column and CD56 microbeads human kit (Miltenyi Biotec (MBio)), according to the manufacturer's instructions. After depleting CD3+ cells from PBMCs using the CD3 microbead human kit and LD MACS separation column, NK cells were cultured in NK MACS medium, 5% human AB serum, 140 UI/mL IL-15 and 500 UI/mL IL-2 (MBio).

Flow Cytometry

For cell phenotyping, the antibody incubation was performed at 4°C in the dark for 20 min in MACS buffer (MBio) supplemented with 0.5% human AB serum. For MB phenotype assessment, conjugation, FACS Canto I (BD) flow cytometer and FACSDiva 6.0 analysis software (BD) were used, and for cytotoxicity assays, MACSQuant10 flow cytometer and Flowlogic (Inivai Technologies) data analysis software. All antibodies used are described in the Supplementary Materials.

Tumour Cell Conjugation Assays

The conjugation of MB and NK cells was assessed using confocal microscopy and flow cytometry. K562 cells were used as positive controls. NK cells were stained for 20 min with CellBrite™ Green (CBG) and Lyso View^{TM} 633 (LV, Biotium), and MB/K562 cells were stained with CellTracker™ Orange (CTO, Thermo Fisher) and then co-cultured at a 2:1 ratio. Finally, the cells were washed, fixed in paraformaldehyde 4% solution and mounted in Fluoroshield (Merck), and imaged using a Leica TCS SP5 X AOBS on an inverted DMI6000 microscope controlled with the LAS AF software (Leica). For the flow cytometry conjugation assay, NK cells were stained with anti-CD56-AlexaFluor488 (BD Biosciences) and MB cell lines with anti-PVR-AlexaFluor647 (BD Biosciences). The cells were then co-cultured in a 1:1 ratio for 15 min. After fixation and washing, the frequency of NK cell/target conjugates was determined as the percentage of CD56+/PVR+ cells.

Degranulation and Intra-Cellular Cytokine Assays

NK cell granzyme B degranulation was assessed using the Granzyme B Elispot Development Module (R&D Systems, USA) according to the manufacturer's instructions. Triplicates with various E:T ratios were seeded at ratios of 100:1, 50:1, and 25:1. Phytohemagglutinin (PHA; Thermo Fisher, USA) was used as a positive control, and NK cells were used as a negative control. After overnight incubation, spot-forming cells (SFC) were counted using a Bioreader 4000 PRO-S (BIO-SYS GmbH, Germany), and the results were expressed per 10^5 NK cells after subtraction of negative control spots.

Cytotoxicity Assays

MB cell necrosis was detected using 7-AAD staining after 4 h of co-culture with NK cells at various E:T ratios. The percentage of experimental necrosis was calculated using the following equation:

$$(\%\ \text{experimental necrosis} - \%\ \text{background necrosis in the negative control})/(100\% - \%\ \text{background necrosis in the negative control})$$

The lysis of MB cells induced by NK cells 24h-co-culture at E:T ratios of 5:1, 2,5:1, 1:1 was assessed using a ToxiLight© bioassay kit (Lonza) according to the manufacturer's instructions. Bioluminescence signals were analysed using a VICTOR X4 (Perkin Elmer). The specific lysis percentage was calculated using the following equation:

$$(\text{Experimental lysis} - \text{background lysis}) \times 100/(\text{Maximal lysis} - \text{background lysis}).$$

Cytokine Array

Chemokines and cytokines in the co-culture and cell line supernatants were detected using the Human Cytokine Antibody Array C3 kit (Raybiotech, USA) according to the manufacturer's instructions. Chemiluminescence imaging was performed using the ChemiDoc© XRS+ system (Bio-Rad, USA), and signals were semi-quantified using ImageJ Software according to the positive control signals. Signals were considered detectable if they were to 2 times superior the background signal intensity.

Medulloblastoma Murine Model

Female nude mice aged six–eight weeks were obtained from Janvier Laboratory (NMRI-nu, Janvier Labs). All in vivo experiments were performed in accordance with institutional and national guidelines and regulations, following the European Community Guidelines (2010/63/UE) for the use of experimental animals with respect of the 3 Rs' requirements for animal welfare. Ethical and legal approval was obtained prior to the commencement of the study: the research project (n°APAFiS #23935) was approved by the French Ministry of Research. Caliper measurements were performed twice weekly for tumour volume calculation (length × width^2)/2), and tumour growth was monitored for 11 weeks or until the tumour volume reached an endpoint of 1000 mm^3. Upon autopsy, the tumours were snap-frozen in liquid nitrogen to extract RNA.

Medulloblastoma Tumour RNASeq

RNA was isolated using the TRIzol Reagent (Invitrogen, USA). PolyA mRNA fractions were enriched using the NEBNext® Poly(A) mRNA Magnetic Isolation Module, and the enriched mRNA fraction was converted to a sequencing library using the NEBNext® Ultra™ II RNA Library Prep Kit for Illumina®. RNASeq was performed in single read SR50 mode on NextSeq2000 at the Epitranscriptomic and Sequencing Core Facility (EpiRNA-Seq) UMS2008 IBSLor and after trimming and alignment to hg19 and mm10 reference genomes, XenofilteR R package was used to differentiate the human transcriptome from the murine transcriptome.[10] Differentially expressed genes (DEG) were analysed using the DESeq2 R package.

Statistics

Statistical analyses were performed using the GraphPad Prism 8 software. NK cell affinity for various MB targets was assessed using the ANOVA test, cytotoxic activity with the *t*-test, and MB tumour progression in animals using the Mann–Whitney test. All results are presented as the mean ± SEM. Statistical significance is shown in the figures with * symbols: *$p<0.05$; **$p<0.01$.

Results

Potential Receptor-Ligand Couples in the Immunological Synapse Between MB and NK Cells

Each MB cell line (DAOY, D283, and D341) was selected to represent various MB subgroups: the SHH group, group 3/4, and group 3, respectively. MB cell lines were examined for the expression of immunomodulatory markers, such as CD73, CD105 (TGF beta receptor), or molecules from the B7 family and NK cell-activating ligands (MICA/B and PVR).

Interestingly, regarding immunomodulatory markers, no significant expression of B7-H1, B7-H3, or B7-H4 was detected, whereas CD73 expression was high and restricted to the DAOY cell line (Figure 1A). CD105, a TGFβ1 receptor, was highly expressed in DAOY cells but was weakly expressed in D341 and D283 cell lines. Regarding the NK cell-activating ligand expressed by MB cell lines, MICA/B, a ligand of NKG2D activating NK cell receptor, was weakly expressed in DAOY and absent in the two other cell lines. PVR (CD155), a DNAM-1 activating ligand, was highly expressed in all three cell lines. This receptor has been shown to correlate with low immune cell infiltration in cancers such as hepatocellular carcinoma.[11]

Cytokine Activation During Expansion Modified NK Cell Phenotype Indicating Maturation and a Greater Functional Potential

To identify NK cell subpopulations that could be present during expansion, we analysed the expression of CD11b (Mac-1), CD27, CD62L, and CD57. The NK cell subpopulations freshly isolated from PBMC were mainly CD11b+ CD27- at baseline (87.5%) (Figure 1B) with a small population of CD11b+CD27+ (9.9%). The latter population decreased overtime, representing 1.5% at D21. The CD11b+ CD27- subpopulation which tended to be stable over time (90.1% at D21), has been described as a subpopulation exhibiting high cytolytic function.[12] Similarly, a subpopulation with an immature CD11b- CD27- phenotype was maintained or even slightly increased over time from baseline (3.5%) until D21

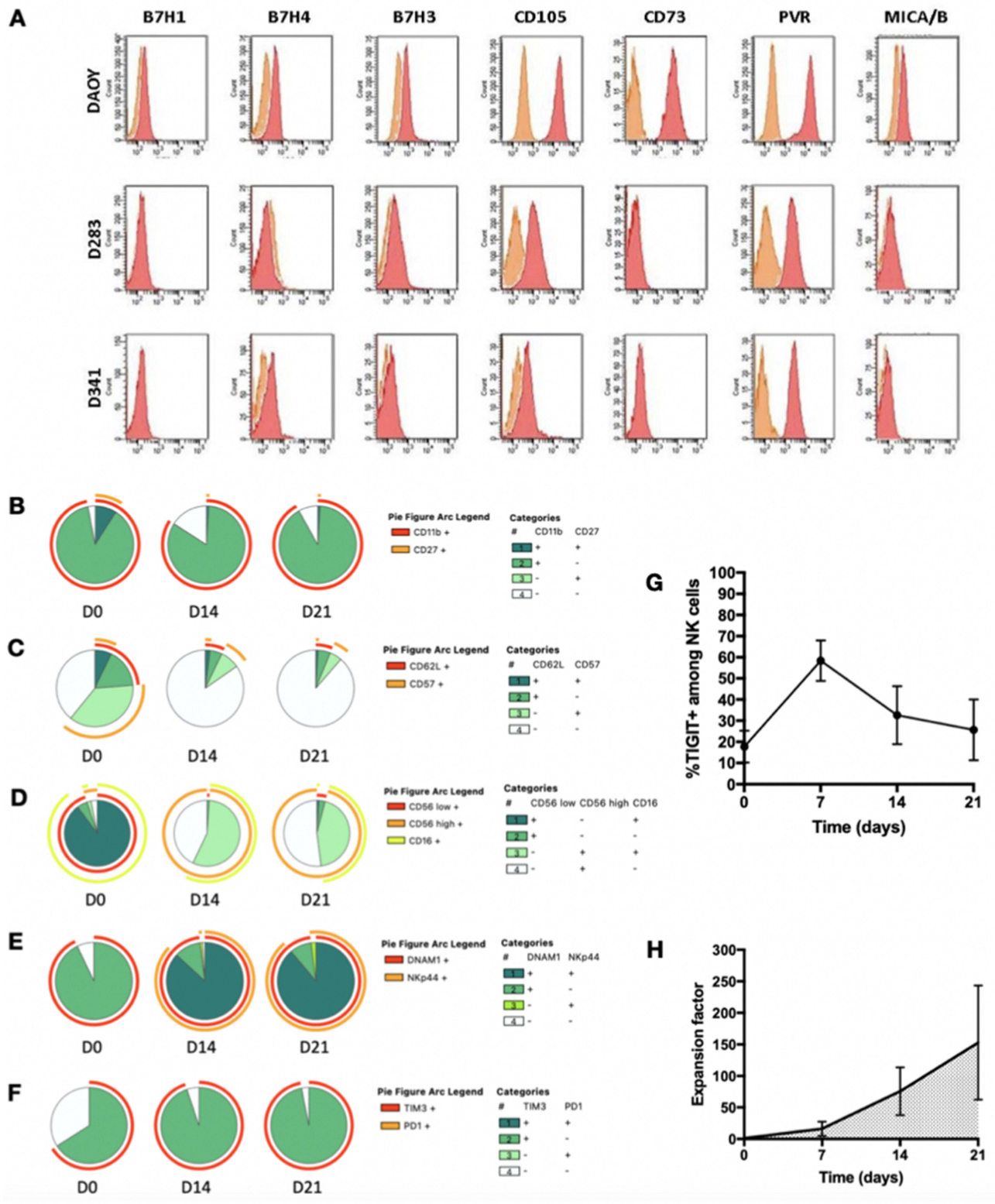

Figure 1 Phenotype analysis of MB cell lines and primary NK cells before and after expansion. (**A**) Immunomodulatory markers and NK cell activating ligands on MB cell lines (pink) and Isotopic controls (Orange). Annotated pie charts showing NK cell phenotype at D0 and during expansion (D14 and D21) regarding (**B**) CD11b and CD27 expression, (**C**) CD62L and CD57 maturation markers, (**D**) CD56high/low and CD16 expression, (**E**) DNAM-1 and NKp44 activating receptors, (**F**) TIM-3 and PD-1 exhaustion markers. (**G**) Percentage of TIGIT+CD56+ NK cells for n=4 representative cultures. (**H**) NK cell expansion factor during expansion period (n=6).

(8.4%) owing to cell proliferation in culture (Figure 1B). The expression levels of both CD62L and CD57 decreased over time (Figure 1C).

Next, we analysed the expression of CD56 and Fcg Receptor, CD16. The percentage of CD56+ NK cells rapidly shifted from CD56 low (9.9% at baseline to 2.2% on day 14) to CD56 high (8.1% at baseline to 97.8% on day 14). In parallel, CD16 expression was downregulated over time from 90.1% at baseline to 51.5% on day 14 (Figure 1D). DNAM-1 was constitutively expressed on NK cells at baseline (92.1%) and remained stable throughout the expansion (97.2% on day 14 and 97.8% on day 21) (Figure 1E). Among the upregulated markers, NKp44, an NCR, increased over time owing to cytokine-activating effects and may be associated with increased cytotoxicity. Regarding exhaustion markers, unlike TIM-3, the expression of PD1 was almost undetectable from baseline to D21 (Figure 1F). Finally, the TIGIT inhibitory receptor, a ligand of PVR constitutively expressed by MB cell lines, reached its highest expression level on day 7 (58.4% versus 17.8% at baseline) (Figure 1G), but then decreased when NK cell expansion started (Figure 1G and H). Altogether, these results suggest a higher direct cytotoxicity potential of expanded NK cells but a decrease in antibody-dependent cell cytotoxicity (ADCC) opportunity.

NK Cells Showed Variable Affinity for Conjugation with MB Target Cells Depending on Their Subgroup and Cytokine Activation

NK cell conjugation and polarisation of the targets were examined using confocal microscopy. The Co-cultured CBG stained NK cells and CTO-stained MB cells demonstrated the ability of NK cells to conjugate with their targets (Figure 2A; upper line). Next, the activation signal led to reorganisation and polarisation of intra-cellular cytotoxic granules

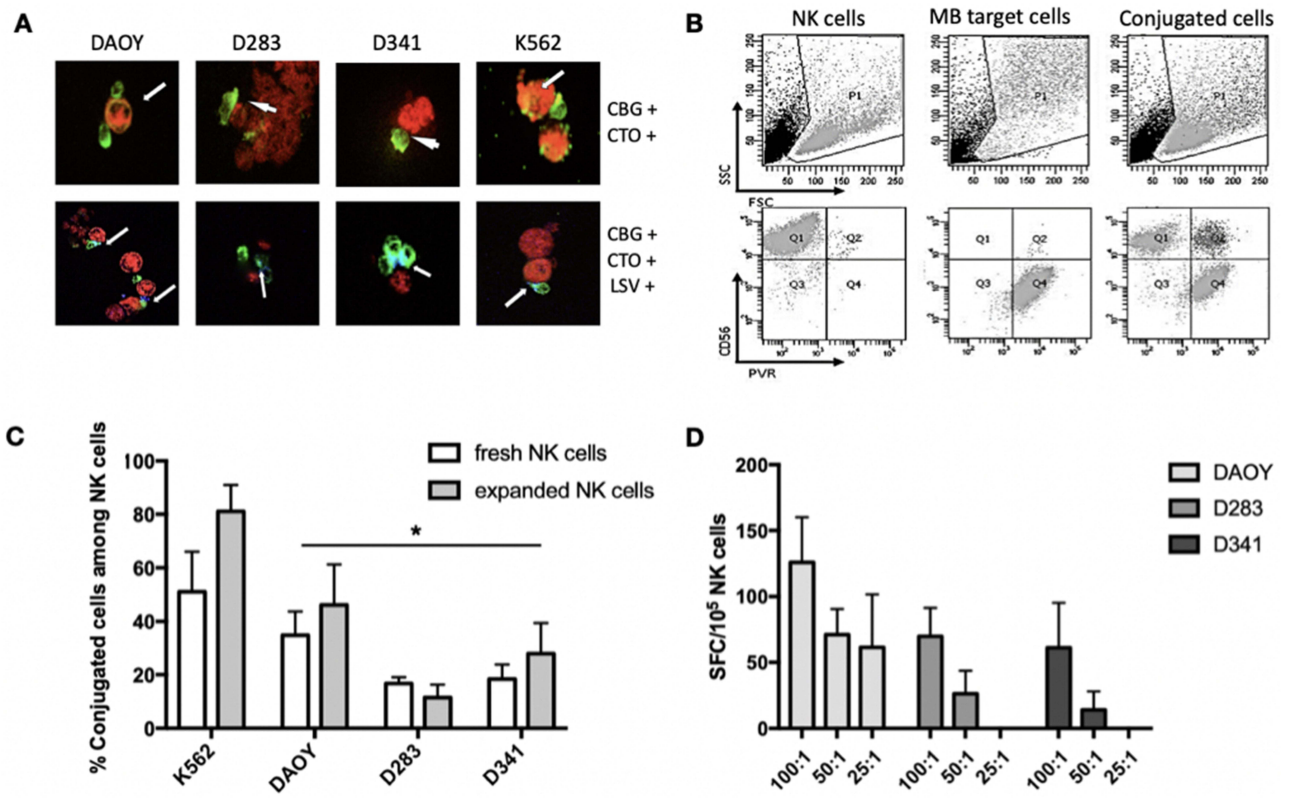

Figure 2 Conjugation, granule polarization and exocytosis as steps of the cytotoxicity mechanism against MB. (**A**) Microscopy imaging (40X) of NK cells conjugation with K562, or MB cell lines. NK cells, target cells and lysosomal granules were respectively stained in green(CBG), red (CTO) and blue (LV). White arrows indicate conjugation area of NK cells with target cells in the upper line, and lysosomal granules polarization in the bottom line. (**B**) Flow cytometry gating strategy showing conjugated cells (CD56+ PVR+) among NK (CD56+) and MB cells (PVR+) co-culture. The upper line shows the FSC/SSC gate excluding cell debris showing NK cells alone (left panel), MB cells alone (middle panel) and conjugates (right panel) and the lower line shows conjugated cells in the CD56+/PVR+ Q2 quadrant. (**C**) Percentages of conjugated NK cells among total (unstimulated) fresh or expanded NK cells with K562, DAOY, D283 and D341 (ANOVA test; * $p<0.05$). (**D**) Expanded NK cells granzyme B secretion after co-culture with MB target cell lines at various E:T ratios (100:1, 50:1, 25:1), ELISPOT results expressed in Spot Forming Colony (SFC) per 10^5 NK cells (n=3).

toward the target cell. Addition of the lysosomal fluorescent marker LysoView allowed us to observe NK cell polarisation to targets with a concentration of lysosomal granules in the contact area (Figure 2A, bottom line). The ability of NK cells to conjugate with MB was assessed using the gating strategy shown in Figure 2B. NK cells showed variable abilities to conjugate to target cells depending on the MB cell line (ANOVA p<0,05 for expanded NK cells). Thus, NK cells had the highest conjugation rate with DAOY cells (34.7% ± 9.1% and 46.1% ± 15.2% for fresh and expanded NK cells, respectively), followed by D341 cells (18.3% ± 5.5% and 27.9% ± 11.5%, respectively) and D283 cells (16.67% ± 2.3% and 11.43% ± 4.8%) (Figure 2C). Moreover, cytokine activation during expansion tended to increase the conjugation rate of NK cells with DAOY and D341 (+32.8% and +52.5%, respectively), but not with D283 (−31.4%).

NK Cell Conjugation to Medulloblastoma Target Cells Induced Granzyme B Exocytosis

Cytotoxicity involves the release of the cytotoxic granules. DAOY cells elicited the highest granzyme B secretion compared with D341 and D283 cells, with a mean of 71 SFC/10^5 NK cells (± 19.6), 14 SFC/10^5 NK cells (± 14) and 26.3 SFC/10^5 NK cells (± 17.3), at 50:1 ratio respectively (Figure 2D). Surprisingly, D341 and D283 cells induced similar ranges of granzyme B secretion despite their different affinities for conjugation to NK cells.

The Secreted Chemokines During NK Cell and MB Cell Co-Culture are Mainly Associated with Angiogenesis and Immune Cell Recruitment

Next, we explored the mediators released by MB and NK cells during the co-culture using a cytokine array (Figure 3A). In the MB cell line secretome, D283 and D341 culture supernatants were poorly enriched with the release of mainly EGF, EGF, and angiogenin, whereas DAOY cells significantly secreted CXCL-1, MCP-3, and IL-6 (Figure 3B). These cytokines are known to promote cell proliferation via activation of the STAT3 axis by IL-6,[13] angiogenesis, and stromal cell recruitment in the TME (tumoral microenvironment) by MCP-3[14] and CXCL-1.[15] Interestingly, these 3 mediators were less frequently expressed after co-culture with NK cells (Figure 3C). IL-6, IL-8, IL-13, IL-15, CXCL-5, MCP-1, RANTES, and GM-CSF were detected in all

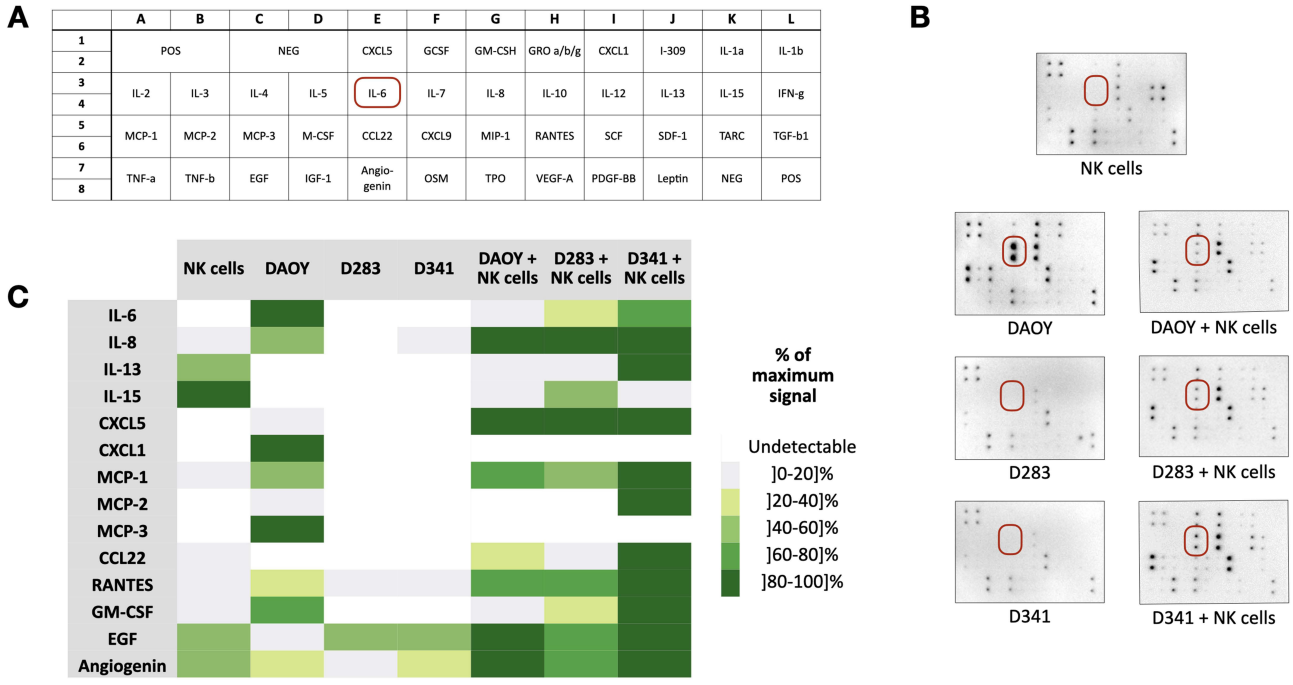

	A	B	C	D	E	F	G	H	I	J	K	L
1	POS		NEG		CXCL5	GCSF	GM-CSH	GRO a/b/g	CXCL1	I-309	IL-1a	IL-1b
2												
3	IL-2	IL-3	IL-4	IL-5	IL-6	IL-7	IL-8	IL-10	IL-12	IL-13	IL-15	IFN-g
4												
5	MCP-1	MCP-2	MCP-3	M-CSF	CCL22	CXCL9	MIP-1	RANTES	SCF	SDF-1	TARC	TGF-b1
6												
7	TNF-a	TNF-b	EGF	IGF-1	Angio-genin	OSM	TPO	VEGF-A	PDGF-BB	Leptin	NEG	POS
8												

Figure 3 Cytokine Array analysis of NK cells and MB cells during co-culture. (**A**) Cytokines detected by membrane array analysis. On each membrane, negative and positive control spots have two to four repeats in upper right and lower left corner. The average intensity of duplicates of the 42 factors was normalized to negative controls. (**B**) Raw cytokine array membrane after incubation with conditioned medium from NK cells or MB cells, or from 24h co-culture. Underlined cytokine spots are IL-6 secretion spots. (**C**) heatmap of 14 most secreted cytokines expressed as percentage of the maximal signal intensity.

the cocultures. IL-8, CXCL5, and RANTES levels were detected after co-culture with NK cells. The highest levels of IL-6, IL-13, MCP-1, MCP-2, CCL22, RANTES, and GM-CSF were detected in the D341/ NK cell supernatant.

NK Cell Cytotoxicity Induced MB Cell Death in 2D Co-Culture Models

The next step in NK cell activation following target cell conjugation is cellular cytotoxicity, which begins with the induction of necrosis of target cells and ends with target lysis. The expanded NK cells had a significantly higher capacity to induce DAOY and D283 necrosis than the fresh unstimulated NK cells (47% versus 27.2% and 38.6% versus 20% for DAOY and D283, respectively; *t*-test, *$p<0.05$) (Figure 4A). However, no significant difference was observed between expanded and fresh NK cells with respect to D341 necrosis after coculture. The highest percentage of necrosis was observed using DAOY cells as targets, and was significantly different from that observed with D341, but not D283 (47% and 31.2%, respectively; *$p<0.05$). Regarding target cell lysis, as detected by the release of adenylate kinase in the co-culture supernatant, D341 and D283 target cell lysis was significantly higher than that of DAOY lysis at an E:T ratio of 5:1 (54%, 60.7%, and 31.2%, respectively; *$p<0.05$, Figure 4B). Taken together, these results show that the MB cell lines have different susceptibilities to NK cell lysis.

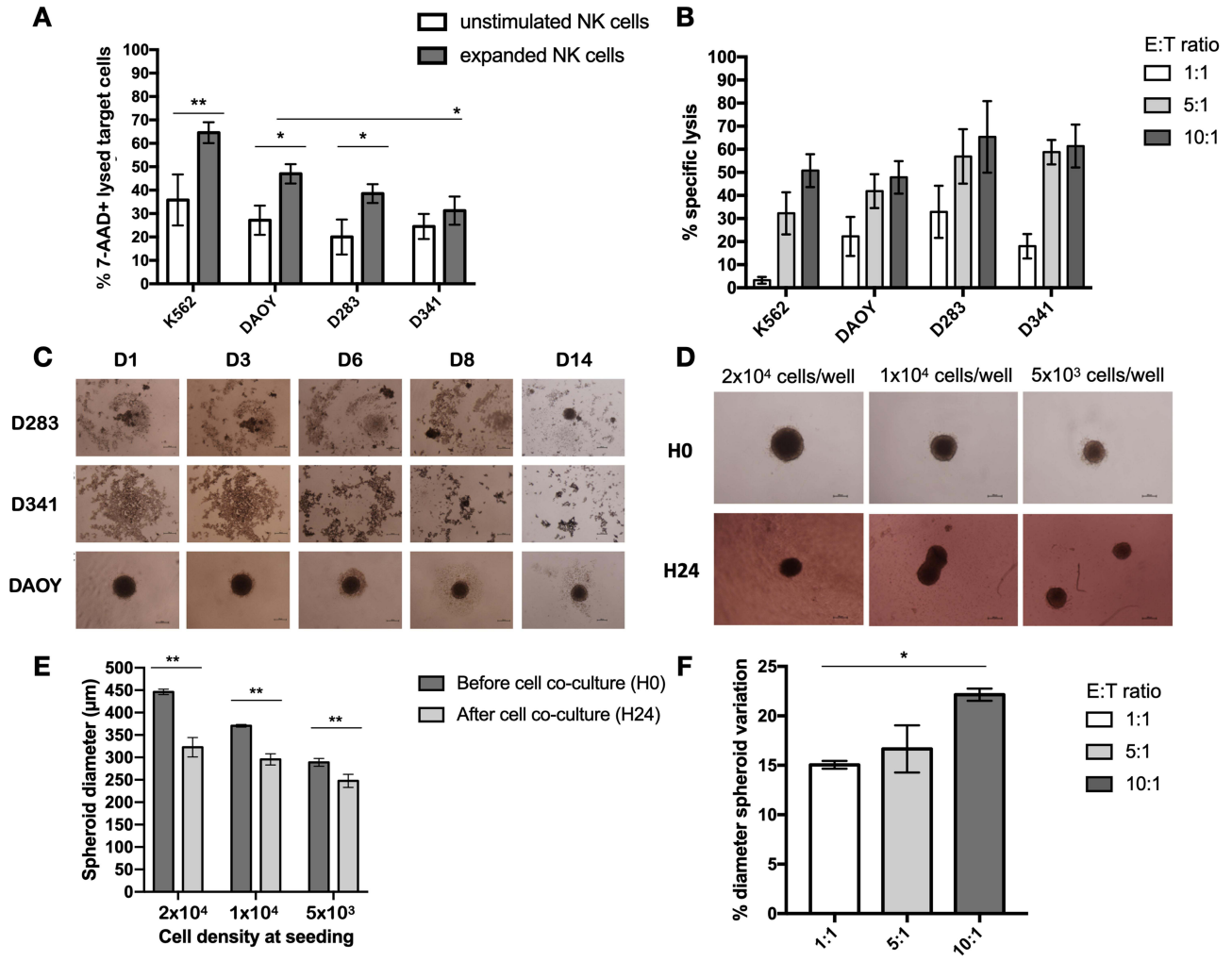

Figure 4 Cytotoxic activity of NK cells in 2D and 3D DAOY spheroid co-culture models. (**A**) Quantitative analysis by flow cytometry of DAOY, D283 and D341 necrosis induced by unstimulated or expanded NK cells at a 5:1 (E:T ratio. K562 is used as a control. (**B**) Quantitative analysis by bioluminescence of specific lysis induced by expanded NK cells in co-culture with the 3 MB cell lines at various (**E**)T ratios. (**C**) Follow-up of spheroid formation during 14 days after 10^4 DAOY cells/well seeding, imaged by inverted microscopy (4X, scale 250µm). (**D**) Spheroid imaging, seeded at various cell densities before (H0) and after (H24) co-culture with expanded NK cells at 10:1 (**E**)T ratio. (**E**) Spheroid diameter (µm) variation after NK cell co-culture at 10:1 (n=7). (**F**) Diameter variation (µm) of 1×10^4 seeded DAOY cell spheroid after 24h of co-culture with expanded NK cells at various (**E**)T ratios (n=4). (*t* test, * p<0.05; ** p<0.01).

Expanded NK Cell Cytotoxicity Achieved Partial DAOY Spheroid Destruction in 3D Co-Culture Model

However, two-dimensional co-culture models are oversimplified for studying immune and tumour cell interactions. Thus, 3D spheroid models can provide more insight into the antitumour activity of NK cells. DAOY spheroids were successfully generated within 24 h, whereas no spheroids were obtained using the D341 or D283 cell lines, even after 14 days of culture (Figure 4C). Therefore, DAOY was selected for the subsequent experiments. Three days after seeding, the diameter of DAOY spheroids was 446± 6µm, 370± 2.8µm and 289± 8.7µm according to a cell seeding density of 2×10^4 cells, 1×10^4 cells, and 5×10^3 cells per well, respectively (Figure 4D and E). After 24 h of co-culture with expanded NK cells at an E:T ratio of 10:1, the spheroid diameter decreased significantly by −27.7% at 2×10^4 cell seeding density, −20.2% at 1×10^4 cell seeding density and −14.2% at 5×10^3 cell seeding density (Figure 4E) owing to DAOY cell lysis by effector cells (** $p<0.01$). In addition, a significant decrease in spheroid diameter was observed when the E:T ratio was increased (−15% at 1:1 E:T versus −22.1% at 10:1 E:T) (* $p<0.05$) (Figure 4F).

Adoptive NK Cell Infusions Significantly Slowed Down Tumour Progression and Increased Overall Survival Rate in Mice

We next assessed whether the adoptive transfer of expanded human NK cells could target MB in vivo. As the DAOY cell line easily forms spheroids and is susceptible to NK cell cytotoxicity, it was chosen to establish subcutaneous xenografts. Ex-vivo expanded NK cells were infused using the caudal vein of mice to be as close as possible to the intravenous infusion that patients would undergo if they were treated with NK cell immunotherapy. In addition, adoptive NK cell development and survival were promoted by injection of human IL-15 (Figure 5A). Thus, IL-15 is central to the survival, growth, and cytotoxicity of NK cells. Twenty-eight days after NK cell infusion, tumour volumes appeared to be significantly higher ($p<0.05$, Mann–Whitney test) in the control group than in the NK group (Figure 5B). Tumour regrowth was observed after this date, although the growth curve remained below that of IL15 and control groups. The control group was euthanised by day 45 due to rapid tumour progression whereas the IL15 and NK groups were euthanised due to maximal tumour volume reached day D80. The median survival time was prolonged by 87% in the NK group (73 days) compared to that in the control group (39 days) and by 69% in the NK group compared to the IL15 group (43 days) (Figure 5C).

In vivo Persistence and Proliferation of Adoptive Activated Human NK Cells Was Detected in the Mice

As NKp44 was highly expressed in ex-vivo expanded NK cells (Figure 1B), this marker was chosen to follow human cells in animals. NK cell persistence was detected throughout the study (~80 days) in the NK cell group (Figure 5D) and was sustained by recurrent administration of IL-15. Notably, no significant proliferation of murine residual Ly49+ NK cells was observed in IL-15 treated animals (Figure 5E). In addition, the Ly49+ NK cell frequency was significantly lower in the NK group than in the IL-15 group, suggesting that human IL-15 promoted human adoptive NK cell persistence better than its murine counterparts.

IL-15 Infusions Do Not Significantly Impact MB Transcriptomic Profile

To determine whether NK cells could modify the gene expression pattern of human MB, tumour samples were subjected to transcriptome analysis (Figure 6). Comparison of the control and IL-15 groups did not reveal any DEG (adjusted $p<0.05$). Subsequent analysis of Gene Ontology (GO) and Kyoto Encyclopedia of Genes and Genome (KEGG) pathway enrichment indicated minor differences between these two groups, as only a few pathways were either up-or down-regulated, with relatively low p-values (data not shown). These results suggested the absence of major remodelling of the MB by human IL-15 injections.

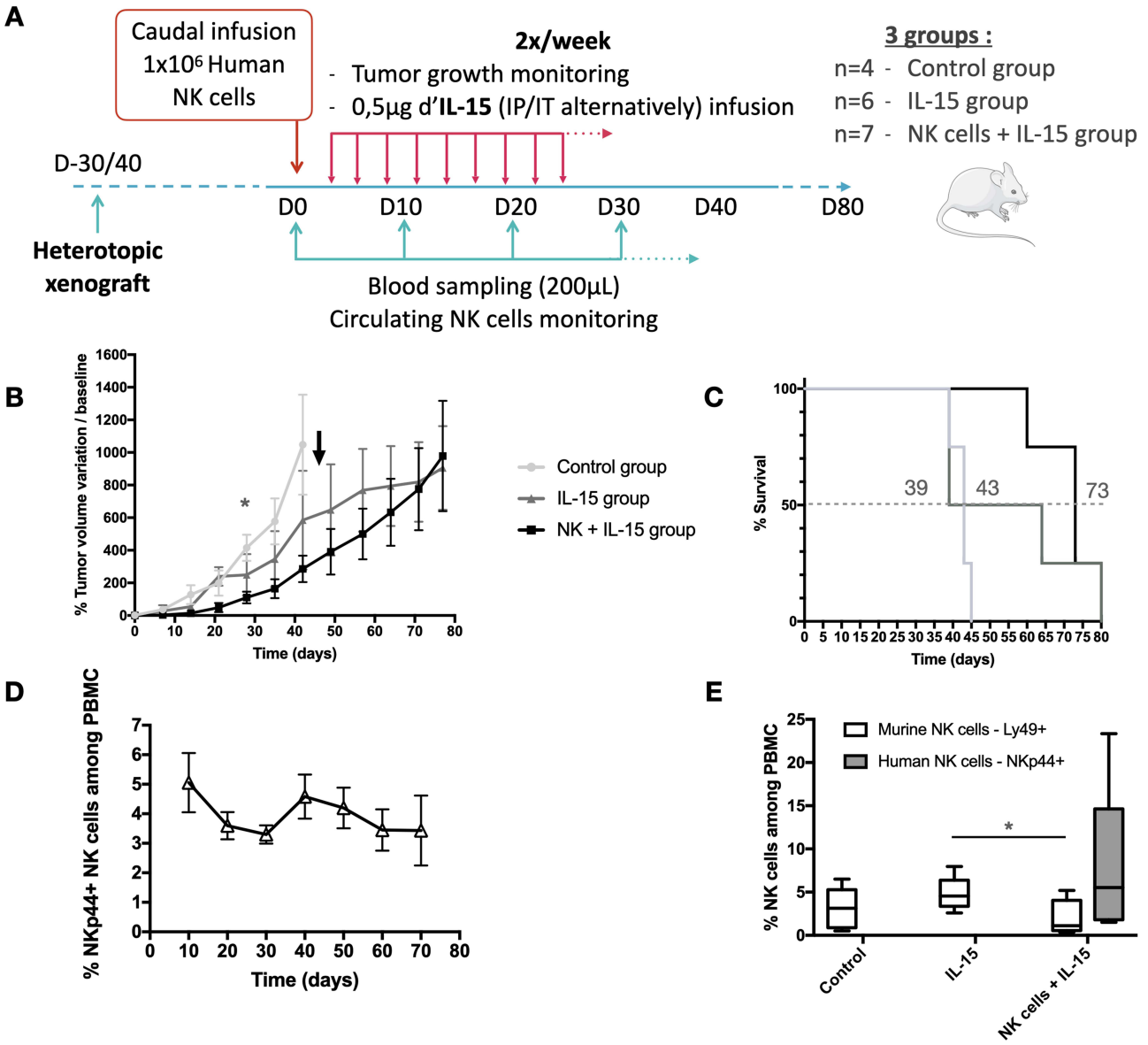

Figure 5 Effect of NK cell adoptive transfer in mouse MB xenograft model (**A**) Experimental design of in vivo study. Mice were randomized in control group (n=4), IL-15 group (n=6) and NK group (n=7) when tumor reached 100 mm3. Following human NK cells (NK group) or saline solution (control and IL-15 group) infusion at day 0, the tumour volume was assessed twice a week with an alternate infusion of 0,5µg intra-tumour or intraperitoneal recombinant human IL-15 (IL-15 and NK group) until animals reached the end-point or day 80 (study's end). Blood samples were withdrawn every 10 days to follow circulating NK cells percentages by flow cytometry. (**B**) Percentage of tumour volume variation from baseline over time. The * indicates the point from which the tumour volume in the NK group became significantly lower than in the control group (D28) ($p<0.05$, Mann–Whitney test). Black arrow indicates the day when the median survival of IL-15 group animals was reached, inducing an inflexion in mean tumour volume progression. (**C**) Kaplan-Meier survival curve. (**D**) Follow up of activated human NK cells (NKp44+) among PBMC in NK group. (**E**) Murine (Ly49+) and NKp44+ NK cells percentage at end-point (*t* test; * $p<0.05$).

Adoptive Human NK Cells Infiltrated MB in vivo, Initiated an Inflammatory Response, Modulating the MB Cells Transcriptome

In contrast, comparative analysis of NK versus the control group and NK versus IL-15 group revealed major perturbations in the human MB cell transcriptome. More than 50 DEG were detected (adjusted p-value <0.05)(Figure 6A). In addition, many of these DEGs showed substantial dysregulation (log2FC>1) (Figure 6B). These results clearly indicate that NK cells substantially modulate the transcriptome of human MB cells.

Analysis of DEGs for the NK versus control and IL-15 groups revealed 15 altered common KEGG pathways, 12 upregulated (Figure 6C and D respectively) and 3 downregulated (Figure 6E and F respectively), indicating the specific

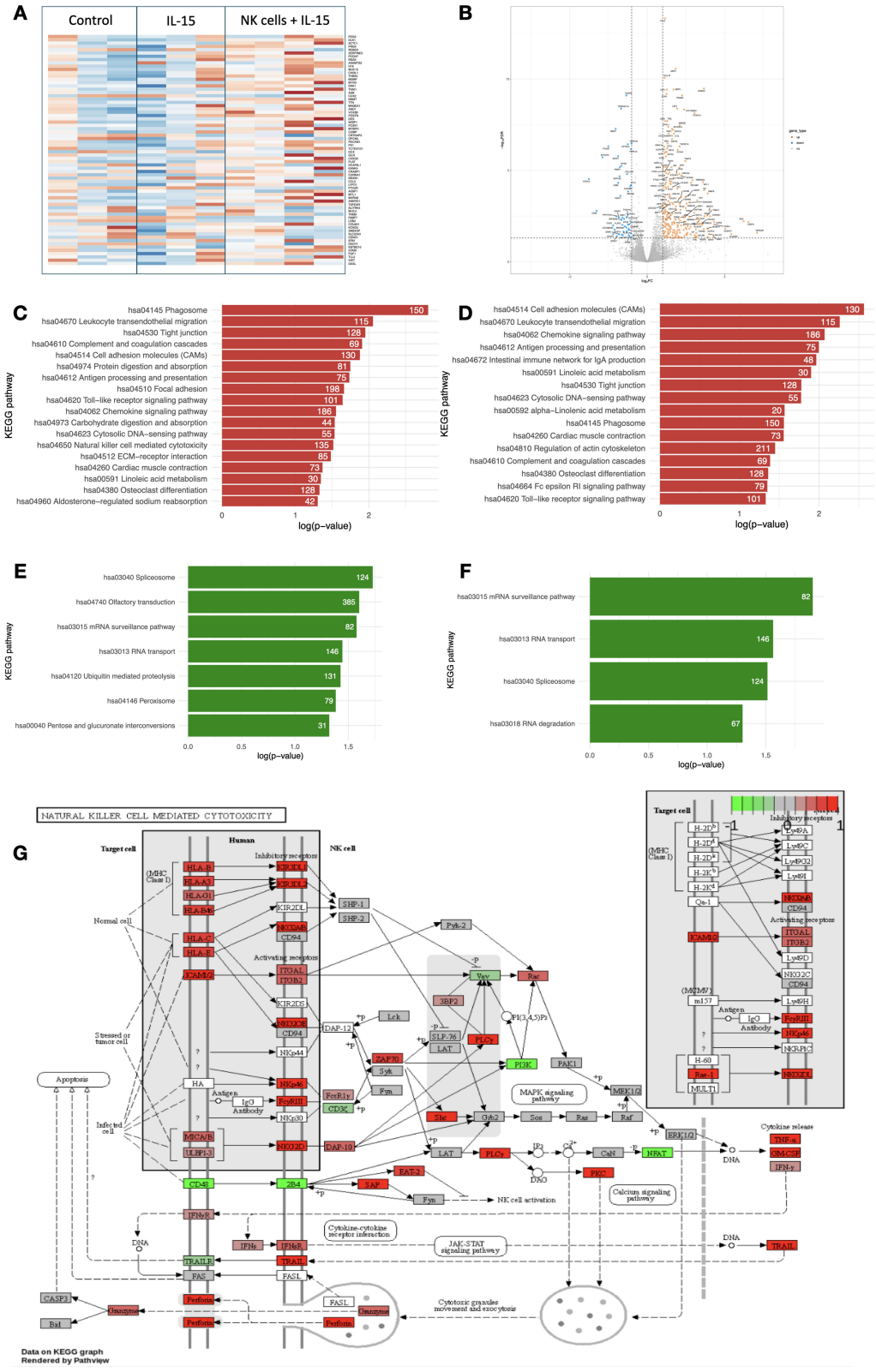

Figure 6 Human transcriptome analysis of tumour samples. (**A**) Vulcano plot of DEG identified between NK and control group (adjusted p value<0.05). (**B**) Heat-map illustrating Up-regulated (red) and down-regulated DEG (blue) according to each group (log2FC>1). (**C**) (**D**) Up-regulated KEGG pathways identified between NK and control group and between NK and IL-15 group. (**E**) (**F**) Down-regulated KEGG pathways identified between NK and control group and between NK and IL-15 group. (**G**) NK cell mediated cytotoxicity pathways (hsa04650, Pathview).

impact of NK cell immunotherapy on the inflammatory response in MB. More precisely, the 12 commonly upregulated pathways were involved in the expression of immune cell adhesion molecules, leukocyte trans-endothelial migration (MLC / TEC / ITGAL / CXCR4 / ICAM1 /PLC/ CDH5/ MMP / CAM), tight junctions, chemokine signalling, antigen processing and presentation, phagosomes, complement and coagulation cascades, and toll-like receptor signalling. Notably of note that 2 up-regulated KEGG pathways were consistent with the SHH MB standard transcriptome and linked to cardiac muscle contraction and osteoclast differentiation. Regarding metabolic pathways, upregulated DEGs were involved in protein and carbohydrate digestion and absorption.

Finally, three common KEGG pathways, involved in spliceosome function, mRNA surveillance, and RNA transport, were downregulated.

Adoptive Human NK Cells Infiltrate the MB Tumour, Activate and Exert Significant Cytotoxic Activity in vivo

Interestingly, when comparing the NK and control groups, DEGs were detected in pathways involved in NK cell cytotoxicity and activation (Figure 6G). These upregulated genes were activating receptors, such as NKG2D, FcgR, and NKp46, and inhibitory receptors, such as KIR3DL1, 3DL2, and NKG2A. Genes involved in cellular signal transduction (zap70, PLC, Shc, and PKC), lysosome formation (lamp, NOS, vATPase, and MPO), and NK cell mediator synthesis (IFNγ, TNFα, GM-CSF, perforin, and granzyme) were also upregulated. Downregulated DEGs included 2B4, CD3zeta, and NFAT.

These results confirmed the NK cell cytotoxicity observed in vitro and in vivo against MB.

Discussion

Here, we explored the cytotoxic properties of natural killer (NK) cells, emphasising their potential as effectors of immunotherapy against MB. While NK cells have demonstrated promise in other brain tumours, such as glioblastoma, there are limited data on MB. Therefore, this study aimed to understand the key steps of NK cell cytotoxicity against MB and evaluate their anti-tumour response using a murine model.

To study the conjugation and activation steps, we first explored the expression of main NK cell ligands on the tumor cell lines and extend our interest in molecules potentially involved in MB immunomodulation. According to results of Castriconi et al, we showed that MB cells indeed express ligands leading to NK cell activation during the immunological synapse.[8] The NKG2D receptor is one of the major activating receptors of NK cells and presents different ligands such as MICA/B. Surprisingly, MICA/B was not significantly expressed on the surface of DAOY, D283 and D341 lines in our in vitro model, contrasting with previously published data.[8] The expression of MICA/B was found on MB cells from patients, suggesting a potential positive regulation of this receptor in vivo in the TME and promoting the lytic activity of NK cells.

Also in vivo, the absence of MICA/B or its shedding[16] has been linked to tumour cell resistance to NK cell cytotoxicity.

Regarding immunomodulatory molecules, we focused our interest on the B7 family. Upon the 3 different cell lines, DAOY cells were found positive for B7H3 and B7H4. B7H3, also known as CD276, is an important checkpoint molecule highly expressed in medulloblastoma[17] with an inhibitory function on T and NK cell activation.[18] Despite its receptor is yet to be discovered, clinical trials are currently ongoing, evaluating the monoclonal antibody omburtamab against B7H3.[17]

We showed also for the first time, that DAOY cells unlike D341 and D283 cells significantly expressed CD105. This marker has been identified as a poor prognosis marker,[19] in many solid cancers, and also its expression reflects a strong angiogenic potential of the tumor associated with dissemination and tumor progression. Additionally, pro-angiogenic factors, such as CXCL-8[20] and angiogenin, were detected after co-culture with NK cells. Interestingly, the expression of CD105 is correlated with the secretion of VEGF in the TME, making it possible to consider an effective anti-angiogenic therapeutic strategy in this situation.

We also demonstrated the expression of PVR on DAOY, D283 and D341 cells confirming the results obtained by Marques et al on tumor samples.[17] The activating DNAM-1 and inhibitory TIGIT receptors are likely to interact with PVR, generating into NK cells, an activating or inhibitory signal, respectively. The impact of PVR expression by tumor cells is therefore ambivalent, but is more readily associated with an inhibitory effect in the context of the TME.[21]

Interestingly, we observed that during NK cell expansion period in presence of IL-15 and IL-2, a high expression level of DNAM-1 was detected whereas TIGIT, although rising at day 7, dropped its expression as soon as NK cell expansion started. This suggested in our setting, that PVR expressed by MB cells interact mainly with the activating receptor DNAM-1 rather than TIGIT.

Of note, by comparing freshly isolated and expanded NK cells, we found that cytokine stimulation had no significant impact on the initial cell conjugation stage.

Regarding the next step, which is target cell lysis induced by NK cell cytotoxicity, we showed also that NK cells exhibit variable cytotoxic activity depending on the MB lineage, and at all stages of the process leading to cell lysis. At initiation, we observed a greater potential for conjugation and induction of granzyme B secretion by NK cells with DAOY cells compared to D341 and D283 cells. Then, our results seemed to indicate that MB cells can be destroyed by NK cells through different modes of independent cytotoxicity leading either preferentially to brutal cell lysis (necrosis) for D341 and D283 cells (Figure 4B), or to a cell death by induction of apoptosis for DAOY cells (Figure 4A). In light with these observations, it would be interesting to carry out co-cultures of NK cells and MB lines in the presence of TRAIL and Fas-L inhibitors in order to confirm this hypothesis. Of note, we observed that the susceptibility of NK cells to lyse the different MB lineages varied between individuals (data not shown). In addition, NK cell cytotoxicity was enhanced upon cytokine stimulation, particularly regarding granzyme B secretion and cell lysis. This may be related to the upregulation of expression upon cytokine stimulation of activating receptors such as DNAM-1 and NKp44.

Next, in a 3D model of spheroids representing tumour micro-regions, we showed that NK cells exhibited significant cytotoxicity against DAOY cells, confirming the results obtained by Roper et al,[22] and consistent with the 2D model results.

The anti-tumour activity of NK cells was confirmed in vivo, leading to reduced tumour progression and increased animal survival in the NK cell group compared to the control group. IL-15 injections supported human NK cell persistence, although their effect on murine NK cells was limited. However, we acknowledge the limitations of the heterotopic mouse model, which prevents NK cells from crossing the blood-brain barrier (BBB) to reach the tumour site. They highlighted previous studies suggesting that MB cells could modulate BBB permeability, making the tumour more or less accessible to treatments and immune effectors. Indeed, regardless of their subtype, MB is characterised by a very weak immune infiltrate, making it impossible to be considered as a prognostic factor for the progression of the disease.[23] However, Phoenix et al showed that MB cells can modulate the permeability of the BBB through paracrine effects, making the tumour more or less accessible to treatments and immune effectors.[24] Furthermore, the BBB obstacle may be easily overcome when treating patients because the feasibility of in situ methods of administration, such as directly into the cerebellum[25] or in the ventricles[26] (NCT02271711), has already been evaluated.

In summary, this study provides insights into the cytotoxicity of NK cells against MB and highlights their potential for immunotherapy opening avenues for future research and clinical applications. Furthermore, these findings support the further exploration of strategies to enhance the native anti-MB potential of NK cells, including approaches involving cytokine stimulation, monoclonal antibodies or genetic modifications.[27] Indeed, NK cells have already proven to be a suitable alternative source to T cells for the development of CAR immunotherapies. Contrary to T cells, NK cells do not require antigen pre-sensitization to lyse target cells. The effectiveness of CAR-NK has currently been demonstrated in vitro against solid cancers such as breast cancer, where they induced fewer off-target effects than their CAR-T cell counterpart thanks to the balance of activating/inhibitory receptors preserving healthy tissues from the action of CAR-NK.[28] In clinical setting against B-cell hematological cancers (non-Hodgkin's lymphoma or chronic lymphocytic leukemia) a high tolerance of CAR-NK immunotherapy without adverse events of cytokine release syndrome type was observed, in contrast to the known toxicity profile of CAR-T cell immunotherapy.[29] The great heterogeneity of expression of activating and inhibitory receptors on their surface induces a very complex regulation of NK cell activity. Thus, the expression profile of activating and inhibitory ligands and the specific resistance mechanisms of each type of tumor cells currently make our results impossible to be extrapolated to other types of cancer. A specific assessment must then be carried out for each potential therapeutic indication in order to assess the potency of NK cells. Exploration of the therapeutic potential of NK cells must therefore be continued, because these cells should become a key player in the panorama of anticancer immunotherapies in the future.

Acknowledgments

We thank Dr. V. Marchand EpiRNA-Seq Core Facility, UMS2008 IBSL or UL-CNRS-INSERM, and Pr. Y. Motorin and IMoPA UMR7365 UL-CNRS for fruitful discussions, experimental protocols, and bioinformatics analysis.

Funding

This work was supported by the Ligue Contre le Cancer (CCIR Est) and Regional Grand-Est projects, EpiARN.

Disclosure

The authors report no conflicts of interest in this work.

References

1. Gerber NU, Mynarek M, von Hoff K, Friedrich C, Resch A, Rutkowski S. Recent developments and current concepts in medulloblastoma. *Cancer Treat Rev*. 2014;40(3):356–365. doi:10.1016/j.ctrv.2013.11.010
2. Menyhárt O, Győrffy B. Molecular stratifications, biomarker candidates and new therapeutic options in current medulloblastoma treatment approaches. *Cancer Metastasis Rev*. 2020;39(1):211–233. doi:10.1007/s10555-020-09854-1
3. Taylor MD, Northcott PA, Korshunov A, et al. Molecular subgroups of medulloblastoma: the current consensus. *Acta Neuropathol*. 2012;123(4):465–472. doi:10.1007/s00401-011-0922-z
4. Taylor RE, Bailey CC, Robinson K, et al. Results of a randomized study of preradiation chemotherapy versus radiotherapy alone for nonmetastatic medulloblastoma: the International Society of Paediatric Oncology/United Kingdom Children's Cancer Study Group PNET-3 Study. *J Clin Oncol*. 2003;21(8):1581–1591. doi:10.1200/JCO.2003.05.116
5. Esfahani K, Roudaia L, Buhlaiga N, Del Rincon SV, Papneja N, Miller WH. A review of cancer immunotherapy: from the past, to the present, to the future. *Curr Oncol*. 2020;27(Suppl 2):S87–S97. doi:10.3747/co.27.5223
6. Wang Y, Zhou C, Luo H, et al. Prognostic implications of immune-related eight-gene signature in pediatric brain tumors. *Braz J Med Biol Res*. 2021;54(7):e10612. doi:10.1590/1414-431X2020e10612
7. June CH, O'Connor RS, Kawalekar OU, Ghassemi S, Milone MC. CAR T cell immunotherapy for human cancer. *Science*. 2018;359(6382):1361–1365. doi:10.1126/science.aar6711
8. Castriconi R, Dondero A, Negri F, et al. Both CD133+ and CD133- medulloblastoma cell lines express ligands for triggering NK receptors and are susceptible to NK-mediated cytotoxicity. *Eur J Immunol*. 2007;37(11):3190–3196. doi:10.1002/eji.200737546
9. Fernández L, Portugal R, Valentín J, et al. In vitro Natural Killer Cell Immunotherapy for Medulloblastoma. *Front Oncol*. 2013;3:94. doi:10.3389/fonc.2013.00094
10. Kluin RJC, Kemper K, Kuilman T, et al. XenofilteR: computational deconvolution of mouse and human reads in tumor xenograft sequence data. *BMC Bioinf*. 2018;19(1):366. doi:10.1186/s12859-018-2353-5
11. Liu WF, Quan B, Li M, Zhang F, Hu KS, Yin X. PVR-A Prognostic Biomarker Correlated with Immune Cell Infiltration in Hepatocellular Carcinoma. *Diagnostics (Basel)*. 2022;12(12):2953. doi:10.3390/diagnostics12122953
12. Fu B, Wang F, Sun R, Ling B, Tian Z, Wei H. CD11b and CD27 reflect distinct population and functional specialization in human natural killer cells. *Immunology*. 2011;133(3):350–359. doi:10.1111/j.1365-2567.2011.03446.x
13. Chen X, Wei J, Li C, Pierson CR, Finlay JL, Lin J. Blocking interleukin-6 signaling inhibits cell viability/proliferation, glycolysis, and colony forming activity of human medulloblastoma cells. *Int J Oncol*. 2018;52(2):571–578. doi:10.3892/ijo.2017.4211
14. Liu Y, Cai Y, Liu L, Wu Y, Xiong X. Crucial biological functions of CCL7 in cancer. *PeerJ*. 2018;6:e4928. doi:10.7717/peerj.4928
15. Penco-Campillo M, Molina C, Piris P, et al. Targeting of the ELR+CXCL/CXCR1/2 Pathway Is a Relevant Strategy for the Treatment of Paediatric Medulloblastomas. *Cells*. 2022;11(23):3933. doi:10.3390/cells11233933
16. Xing S, Ferrari de Andrade L. NKG2D and MICA/B shedding: a "tag game" between NK cells and malignant cells. *Clin Transl Immunology*. 2020;9(12):e1230. doi:10.1002/cti2.1230
17. Marques RF, Moreno DA, da Silva L, et al. Digital expression profile of immune checkpoint genes in medulloblastomas identifies CD24 and CD276 as putative immunotherapy targets. *Front Immunol*. 2023;14:1062856. doi:10.3389/fimmu.2023.1062856
18. Khan M, Arooj S, Wang H. NK Cell-Based Immune Checkpoint Inhibition. *Front Immunol*. 2020;11:167. doi:10.3389/fimmu.2020.00167
19. Saroufim A, Messai Y, Hasmim M, et al. Tumoral CD105 is a novel independent prognostic marker for prognosis in clear-cell renal cell carcinoma. *Br J Cancer*. 2014;110(7):1778–1784. doi:10.1038/bjc.2014.71
20. Sparmann A, Bar-Sagi D. Ras-induced interleukin-8 expression plays a critical role in tumor growth and angiogenesis. *Cancer Cell*. 2004;6(5):447–458. doi:10.1016/j.ccr.2004.09.028
21. Kučan Brlić P, Lenac Roviš T, Cinamon G, Tsukerman P, Mandelboim O, Jonjić S. Targeting PVR (CD155) and its receptors in anti-tumor therapy. *Cell Mol Immunol*. 2019;16(1):40–52. doi:10.1038/s41423-018-0168-y
22. Roper SJ, Linke F, Scotting PJ, Coyle B. 3D spheroid models of paediatric SHH medulloblastoma mimic tumour biology, drug response and metastatic dissemination. *Sci Rep*. 2021;11(1):4259. doi:10.1038/s41598-021-83809-6
23. Bockmayr M, Mohme M, Klauschen F, et al. Subgroup-specific immune and stromal microenvironment in medulloblastoma. *Oncoimmunology*. 2018;7(9):e1462430. doi:10.1080/2162402X.2018.1462430
24. Phoenix TN, Patmore DM, Boop S, et al. Medulloblastoma genotype dictates blood brain barrier phenotype. *Cancer Cell*. 2016;29(4):508–522. doi:10.1016/j.ccell.2016.03.002
25. Kennis BA, Michel KA, Brugmann WB, et al. Monitoring of intracerebellarly-administered natural killer cells with fluorine-19 MRI. *J Neurooncol*. 2019;142(3):395–407. doi:10.1007/s11060-019-03091-5

26. Khatua S, Cooper LJN, Sandberg DI, et al. Phase I study of intraventricular infusions of autologous ex vivo expanded NK cells in children with recurrent medulloblastoma and ependymoma. *Neuro Oncol*. 2020;22(8):1214–1225. doi:10.1093/neuonc/noaa047
27. Strecker MI, Wlotzka K, Strassheimer F, et al. AAV-mediated gene transfer of a checkpoint inhibitor in combination with HER2-targeted CAR-NK cells as experimental therapy for glioblastoma. *Oncoimmunology*. 2022;11(1):2127508. doi:10.1080/2162402X.2022.2127508
28. Portillo AL, Hogg R, Poznanski SM, et al. Expanded human NK cells armed with CAR uncouple potent anti-tumor activity from off-tumor toxicity against solid tumors. *iScience*. 2021;24(6):102619. doi:10.1016/j.isci.2021.102619
29. Liu E, Marin D, Banerjee P, et al. Use of CAR-Transduced Natural Killer Cells in CD19-Positive Lymphoid Tumors. *N Engl J Med*. 2020;382:545–553. doi:10.1056/NEJMoa1910607